



1 **Quantifying the soil sink of atmospheric Hydrogen: a full year of field**  
2 **measurements from grassland and forest soils in the UK**

3 Nicholas Cowan<sup>1</sup>, Toby Roberts<sup>1</sup>, Mark Hanlon<sup>1</sup>, Aurelia Bezanger<sup>1</sup>, Galina Toteva<sup>1,2</sup>, Alex Tweedie<sup>1,2</sup>, Karen  
4 Yeung<sup>1</sup>, Ajinkya Deshpande<sup>1</sup>, Peter Levy<sup>1</sup>, Ute Skiba<sup>1</sup>, Eiko Nemitz<sup>1</sup>, Julia Drewer<sup>1</sup>

5 <sup>1</sup>UK Centre for Ecology and Hydrology, Easter Bush, Midlothian, UK, EH26 0QB

6 <sup>2</sup>School of GeoSciences, The University of Edinburgh, Edinburgh, United Kingdom

7 **Corresponding author:** Nicholas Cowan (nicwan11@ceh.ac.uk)

8 **Keywords:** greenhouse gas, carbon, methane, flux, chamber methodology

9 **Abstract**

10 Emissions of hydrogen (H<sub>2</sub>) gas from human activities are associated with indirect climate warming effects. As  
11 the hydrogen economy expands globally (e.g. the use of H<sub>2</sub> gas as an energy source), the anthropogenic  
12 release of H<sub>2</sub> into the atmosphere is expected to rise rapidly as a result of increased leakage. The dominant  
13 H<sub>2</sub> removal process is uptake into soils; however, removal mechanisms are poorly understood and the fate  
14 and impact of increased H<sub>2</sub> emissions remains highly uncertain. Fluxes of H<sub>2</sub> with soils are rarely measured,  
15 and data to inform global models is based on few studies. This study presents soil H<sub>2</sub> fluxes from two field  
16 sites in central Scotland, a managed grassland and a planted deciduous woodland, with flux measurements  
17 of H<sub>2</sub> covering full seasonal cycles. A bespoke flux chamber measurement protocol was developed to deal  
18 with the fast decline in headspace concentrations associated with rapid H<sub>2</sub> fluxes, in which non-linear  
19 regression models could be fitted to concentration data over a 7-minute enclosure time. We estimate annual  
20 H<sub>2</sub> uptake of  $-3.1 \pm 0.1$  and  $-12.0 \pm 0.4$  kg H<sub>2</sub> ha<sup>-1</sup> yr<sup>-1</sup> and mean deposition velocities of  $0.012 \pm 0.002$  and  
21  $0.088 \pm 0.005$  cm s<sup>-1</sup> for the grassland and woodland sites, respectively. Soil moisture was found to be the  
22 primary driver of H<sub>2</sub> uptake at the grassland site, where the high clay content of the soil resulted in anaerobic  
23 conditions (near zero H<sub>2</sub> flux) during wet periods of the year. Uptake of H<sub>2</sub> at the forest site was highly variable  
24 and did not correlate well with any localised soil properties (soil moisture, temperature, total carbon and  
25 nitrogen content). It is likely that the high clay content of the grassland site (55% clay) decreased aeration  
26 when soils were wet, resulting in poor aeration and low H<sub>2</sub> uptake. The well-drained forest site (25% clay) was  
27 not as restricted by exchange of H<sub>2</sub> between the atmosphere and the soil, showing instead a large variability  
28 in H<sub>2</sub> flux that is more likely to be related to heterogeneous factors in the soil that control microbial activity  
29 (e.g. labile carbon and microbial densities). The results of this study highlight that there is still much that we



30 do not understand regarding the drivers of H<sub>2</sub> uptake in soils and that further field measurements are required  
31 to improve global models.

## 32 **1. Introduction**

33 Prior to the industrial revolution in the 18<sup>th</sup> century, the atmospheric concentration of Hydrogen gas (H<sub>2</sub>) was  
34 relatively stable at approximately 330 ppb (Patterson et al., 2021). Human activity over the past two centuries  
35 has resulted in increasing atmospheric H<sub>2</sub> concentrations (546 ppb in 2021, Petron et al. (2023)), partly as a  
36 result of increasing industrial leaks (Hitchcock 2019; Cooper et al., 2022), partly due to increases in emissions  
37 and concentrations of precursor gases such as methane (CH<sub>4</sub>) and volatile organic compounds (VOCs), and  
38 partly due to increasing concentrations of other gases in the atmosphere which extend the natural lifetime  
39 of H<sub>2</sub> (Patterson et al., 2021). In the atmosphere, H<sub>2</sub> competes for hydroxyl (OH) radicals with gases such as  
40 methane (CH<sub>4</sub>) and carbon monoxide (CO), thus an increase in concentrations of these gases due to human  
41 activities has resulted in increasing competition for OH and extended the lifetimes for each species (Khalil &  
42 Rasmussen, 1990; Bertagni et al., 2022). Concentrations of atmospheric H<sub>2</sub> gas are indirectly associated with  
43 climate warming effects as a result of extending the atmospheric lifetime of the powerful greenhouse gas CH<sub>4</sub>  
44 as well as increasing tropospheric ozone and water vapour, which also have a warming potential (Warwick et  
45 al., 2004; Ocko & Hamburg, 2022). The associated indirect global warming potential (GWP) had been  
46 estimated to be in the range of 3.3 to 5 over a hundred-year time horizon (Derwent et al., 2020, Field &  
47 Derwent, 2021), though recent estimates have been made of up to 11.6 ± 2.8 times that of an equivalent  
48 mass of carbon dioxide (Sand et al., 2023). The effective GWP and the atmospheric accumulation of H<sub>2</sub> are  
49 highly sensitive to its atmospheric lifetime, which is estimated to be approximately 2 years (Novelli et al.,  
50 1999).

51 The dominant process for H<sub>2</sub> removal from the atmosphere is uptake by soils, which is estimated to be three  
52 times larger than the sink due to atmospheric reaction with OH (Warwick et al., 2004; Derwent et al., 2020;  
53 Field & Derwent, 2021; Paulot et al., 2021; Ocko & Hamburg, 2022). Whilst both removal mechanisms are  
54 highly uncertain, the fate and impact of increased H<sub>2</sub> emissions depends largely on the soil sink strength  
55 (Ehhalt & Rohrer, 2009). The soil H<sub>2</sub> sink is caused by microbial activity, both under aerobic and anaerobic  
56 conditions (Piché-Choquette & Constant, 2019). A large spectrum of bacteria and archaea can utilise H<sub>2</sub> as an  
57 energy source, via the hydrogenase enzyme. Whilst some investigations have highlighted the importance of  
58 high-affinity H<sub>2</sub>-oxidising bacteria (Saavedra-Lavoie et al., 2020), most studies suggest that this enzyme is  
59 widespread across many bacterial and archaeal phyla, and that H<sub>2</sub> consumption is the norm rather than the  
60 exception (Islam et al., 2020; Greening & Grinter, 2022). It has been suggested that the potential soil H<sub>2</sub> sink  
61 is very large because of the high H<sub>2</sub> demand of microbes (Smith-Downey et al., 2008). However, specific H<sub>2</sub>



62 uptake rates for different soil types and conditions are lacking. In addition to microbial activity, diffusion into  
63 the soil is a further important rate limiting step. Gases penetrate the soil by passive diffusion and diffusion  
64 rates are mainly influenced by porosity, which is affected by soil structure, texture, organic matter contents,  
65 vegetation types (roots) and moisture content. Thus, for the same microbial activity, porous soils can be  
66 expected to be much larger H<sub>2</sub> sinks than compacted and/or waterlogged soils due to increased gas exchange  
67 rates with the atmosphere. At the larger scale, diffusion rates will depend on the changing climate: a wetter  
68 climate may lower the H<sub>2</sub> diffusion rates (Paulot et al., 2021). Temperature is another important factor as it  
69 determines the rate of microbial enzyme reactions, and a carbon source is required for heterotrophic  
70 microbial activity (Islam et al., 2020; Meredith et al., 2016; Baril et al., 2022). In addition, soil H<sub>2</sub>  
71 concentrations will be competing with CH<sub>4</sub> as the energy source for soil microbes, hence the H<sub>2</sub> sink strength  
72 may in turn affect the CH<sub>4</sub> sink strength and vice versa (Conrad, 1999). The biological sink of atmospheric H<sub>2</sub>  
73 has been suggested to be more sensitive to spatial variations of drivers compared to the fluxes of other gases  
74 with high variability such as nitrous oxide (N<sub>2</sub>O); however, H<sub>2</sub> measurement data are limited (Baril et al.,  
75 2022).

76 Historically, the processes that control H<sub>2</sub> uptake in soils have been severely understudied due to the logistical  
77 difficulties and technical constraints on measuring H<sub>2</sub> fluxes. This study presents measurements of H<sub>2</sub> fluxes  
78 between the soil and the atmosphere at two field sites in central Scotland, a managed grassland and a planted  
79 deciduous woodland. These are the first reported flux measurements of H<sub>2</sub> covering a full annual cycle in the  
80 UK. It has previously been reported that forest ecosystems exhibit higher H<sub>2</sub> uptake rates than agroecosystems  
81 (Ehhalt and Rohrer, 2009); however, the generality of this and exact mechanisms are still unclear. This study  
82 aims to investigate the response of microbial H<sub>2</sub> uptake at a grassland and a forest site to environmental  
83 drivers, and to identify differences between the sites. We also describe a dedicated flux chamber  
84 methodology which has been developed to best address the challenges of measuring H<sub>2</sub> flux using gas  
85 chromatography (GC) analysers.

86

## 87 **2. Methods**

### 88 **2.1. Field Sites**

89 Measurements of trace gas fluxes and environmental variables were made at two field sites within the  
90 Midlothian region in central Scotland (UK, approximately 6 miles south of Edinburgh, Table 1). The first of  
91 these was the long-term environmental monitoring site at Easter Bush Farm (grassland). The grassland site  
92 (55.8653 °N, -3.206 °W) is an intensively managed, improved grassland (South field in Cowan et al., 2020 and  
93 Drewer et al., 2016) that since 2001 has been used predominantly to graze sheep, with a species composition



94 of >99% perennial ryegrass (*Lolium perenne*). The soil type is an imperfectly drained Eutric Cambisol with clay  
95 soil. The field management is typical for this region, with predominately ammonium nitrate (AN) fertilisation  
96 via tractor-mounted broadcast spreading, with liming every 3 – 5 years to maintain the pH between 5.5 and  
97 6.0 and occasional ploughing and reseeding. The sheep were absent from the fields in the winter months  
98 (November to February), with sporadic movement between local fields throughout the growing season  
99 (March to September) as management required. During the period of 01/10/23 to 01/10/24, the cumulative  
100 rainfall at the grassland site was 1133 mm and the mean temperature was 8.6 °C which is fairly typical of the  
101 site (Table 1)

102 The second field site was a temporary experimental area setup in Glencorse Forest (woodland). Glencorse  
103 Forest (55.8540°N, -3.215°W) was converted to a planted deciduous forest from a pasture approximately 40  
104 years prior to measurements (Billington and Pelham, 1991). The study plot is situated in a plantation of Silver  
105 Birch (*Betula pendula*) and Downy Birch (*Betula pubescens*), with a ground flora consisting mostly of grasses.  
106 The soil is classified as a sandy loam which lies under a thin layer (5 – 10 mm) of organic debris. The field site  
107 had been subject to enhanced nitrogen deposition with ammonia for approximately 2 years before H<sub>2</sub> flux  
108 measurements were carried out (Deshpande et al., 2024). During the period of 01/10/23 to 01/10/24, the  
109 cumulative rainfall at the woodland site was 1047 mm and the mean temperature was 9.6 °C which was  
110 slightly wetter and warmer than historical mean data (Table 1).

111 **Table 1** Field site environmental properties as reported in previous studies and ongoing research. Mean  
112 annual values taken from 10+ years of site data. Rainfall represents throughfall (e.g. rain that reaches the  
113 soil).

Property	Easter Bush Farm	Glencorse Forest
Management	Improved grassland (grazed)	Planted woodland (Birch)
Abbreviation	Grassland	Woodland
Soil Type	Mineral	Mineral
Carbon Content (% mass)	4.0	3.1
pH	5.5	5.3
Bulk Density (g cm <sup>-3</sup> )	1.11	0.96
Particle Density (g cm <sup>-3</sup> )	2.57	2.34
Sand/silt/clay (%)	25/20/55	60/15/25
Mean Annual Temperature (°C)	8.4	9.0
Mean Annual Rainfall (mm)	1040	920

114

## 115 **2.2. Meteorological and soil measurements**

116 Continuous environmental measurements were made at both field sites. Air temperature, soil temperature,  
117 soil volumetric water content (VWC) at three depths (5, 10 and 20 cm at the grassland site; 5, 10 and 15 cm



118 at the woodland site), relative humidity (RH) and rainfall were measured at both sites throughout the flux  
119 measurement campaign (Table S1). For each flux chamber measurement, soil temperature and soil VWC were  
120 also measured next to the chamber (<0.5 m distance) at the time of the flux measurement. Soil temperature  
121 was measured at 10 cm depth using a handheld probe (ETI Ltd., Worthing, UK), and soil VWC was measured  
122 at 12 cm depth using an HS2 HydroSense II handheld soil moisture sensor (Campbell Scientific, Utah, USA),  
123 with 4 replicates for each chamber. Soil samples were collected for total carbon (C) and total nitrogen (N)  
124 analysis from the top 10 cm of soil at the woodland site in March 2021, September 2021, May 2022, August  
125 2022, November 2022, and March 2023. Subsamples were dried at 105 °C until constant weight, milled using  
126 a ball mill (MM200 ball mill, Retsch, Haan, Germany) and analysed using an elemental analyser (Flash SMART,  
127 Thermo Fisher Scientific, MA, USA).

128

### 129 **2.3. Flux measurements**

130 Fluxes of hydrogen (H<sub>2</sub>), methane (CH<sub>4</sub>) and nitrous oxide (N<sub>2</sub>O) were measured using the static chamber  
131 method (e.g. Drewer et al., 2016). Chambers (diameter = 40 cm, height = 30 cm) consisting of opaque  
132 polypropylene open-ended cylinders, were installed at each field site: 20 at Easter Bush (grassland) and 36 at  
133 Glencorse (woodland). The chambers were inserted into the ground to a depth of approximately 10 cm for  
134 the entire study period. The depth to the surface in each chamber was measured at 5 points on the sides of  
135 the chamber base using a ruler, from which the average was used to calculate the volume of air within. During  
136 measurement periods, aluminium lids were fastened onto the bases using four strong clips; a strip of draft  
137 excluder glued onto the lid provided a gas tight seal between chamber and lid. A three-way tap was used for  
138 gas sample removal using a 100 ml syringe. 20 ml glass vials were filled with a double needle system to flush  
139 the vials with five times their volume. Storage tests using gas standards revealed that gases stored in the vials  
140 were stable for up to 24 hours, after which H<sub>2</sub> leakage could be observed in the data. Hence all analyses of H<sub>2</sub>  
141 gas samples from the chambers were carried out within 24 hours of measurement in the field (typically within  
142 6 hours). Measurements of H<sub>2</sub> and GHGs were made approximately monthly.

143 Two separate measurement protocols were employed to measure greenhouse gases (GHGs) and H<sub>2</sub> fluxes,  
144 due to the differences in how the gases behaved within the chamber over a given timespan. For GHG  
145 measurements, the standard practice of extracting four gas samples (100 ml) at regular intervals over one  
146 hour (0, 20, 40, 60 min) was used (Drewer et al. 2017). However, due to the rapid uptake of H<sub>2</sub> observed in  
147 trial measurements (H<sub>2</sub> in the chamber headspace could reach zero ppb in under 10 mins), the time-evolution  
148 of H<sub>2</sub> in the chamber was non-linear and therefore a separate measurement protocol was developed for H<sub>2</sub>  
149 fluxes. Fluxes of H<sub>2</sub> were measured during entirely separate enclosure periods to the GHGs (albeit on the  
150 same day) using an enclosure period with 6 samples taken over 7 minutes (0, 1, 2, 3, 5 & 7 mins). Chambers



151 used to measure H<sub>2</sub> were fitted with a small 5 cm diameter PC fan which ran from a 9 V battery during chamber  
152 enclosure times to ensure rapid air mixing over the shorter measurement period.

153 Concentrations of H<sub>2</sub> were measured using an Agilent 8890 gas chromatograph fitted with a pulsed discharge  
154 helium ionization detector (GC-PDHID) equipped with a 7697A headspace autosampler, with capacity for 108  
155 vials (Agilent, Santa Clara, California, USA). Concentrations of CH<sub>4</sub> and N<sub>2</sub>O were measured using a gas  
156 chromatograph (Agilent 7890B with headspace autosampler 7697A with capacity for 108 vials; Agilent, Santa  
157 Clara, California, USA) with a micro-electron capture detector (μECD) for N<sub>2</sub>O analysis and flame ionization  
158 detector (FID) for CH<sub>4</sub> analysis run in parallel. Each analytical run of H<sub>2</sub> and GHG samples included at least  
159 three sets of four certified standard concentrations for calibration purposes (certified to ± 5%). The  
160 instrumental noise (σ) of the instruments were 40, 5, and 15 ppb for CH<sub>4</sub>, N<sub>2</sub>O and H<sub>2</sub>, respectively. Based on  
161 the methods used, the analytical uncertainty in flux estimates were 0.38, 0.047 and 1.08 nmol m<sup>-2</sup> sec<sup>-1</sup> for  
162 CH<sub>4</sub>, N<sub>2</sub>O and H<sub>2</sub>, respectively.

163 Fluxes were calculated using linear and non-linear regression methods using the HMR package for the  
164 statistical software R (Pedersen *et al.*, 2010). By convention, positive fluxes represent emission from the soil,  
165 and negative fluxes indicate that the soil acts as a sink. Fluxes of GHGs were all calculated using linear  
166 regression, where  $dC/dt$  is calculated using the standard line of best fit through the concentration data. As  
167 concentrations of H<sub>2</sub> fall exponentially during chamber measurements when soil uptake of H<sub>2</sub> is high, linear  
168 regression is not always appropriate. To account for this, fluxes of H<sub>2</sub> were calculated using both linear  
169 regression and the HM model, depending on the magnitude of the rate of change observed in each chamber  
170 measurement. The HM model is a commonly used non-linear model derived by Hutchinson & Mosier (1981)  
171 with a negative exponential form of curvature which calculates the rate of change of a gas concentration at  
172  $t = 0$ . The concentration  $C$  at time  $t$  is given by Equation 1, where  $C_0$  is the initial concentration,  $C_{max}$  is the  
173 value at equilibrium and  $k$  is a constant.  $dC/dt$  is the initial rate of change in concentration at  $t = 0$  in nmol  
174 mol<sup>-1</sup> s<sup>-1</sup>, calculated using Equation 2.

175 
$$C_t = C_{max} - (C_{max} - C_0) \exp(-kt) \quad (\text{Equation 1})$$

176 
$$\frac{dC}{dt} = k(C_{max} - C_0) \quad (\text{Equation 2})$$

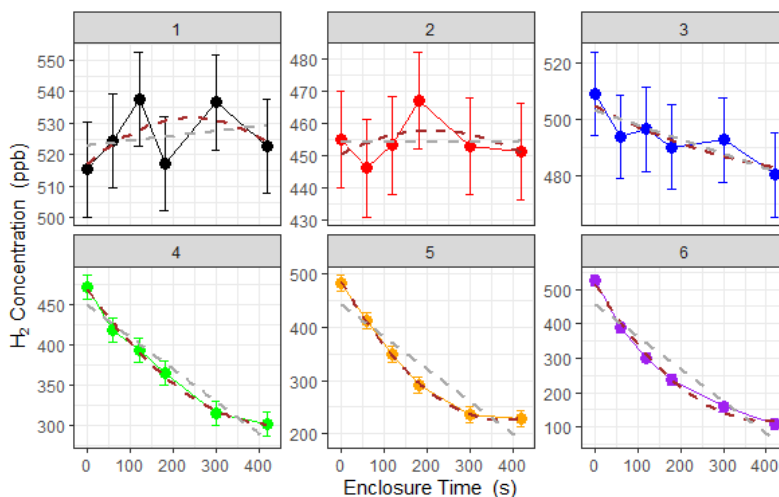
177 The initial  $dC/dt$  is used to calculate the flux using Equation 3, where  $F$  is gas flux from the soil (nmol m<sup>-2</sup> s<sup>-1</sup>),  
178  $\rho$  is the density of air in mol m<sup>-3</sup>,  $V$  is the volume of the chamber in m<sup>3</sup> and  $A$  is the ground area enclosed by  
179 the chamber in m<sup>2</sup>.

180 
$$F = \frac{dC}{dt} \times \rho \times \frac{V}{A} \quad (\text{Equation 3})$$



181 At low concentrations near the limit of detection of the analyser, a clear exponential decline was hard to  
182 discern from the measurement noise and could give rise to spurious fits to Equation 1. (Examples 1 and 2 in  
183 Figure 1 and Table 2). The criteria for using the HM model for each individual flux calculation was based on i)  
184  $k$  is not unrealistically large in Equation 2 (as defined and limited by the HMR package in R), ii) the flux  
185 estimated by linear regression is larger than the analytical uncertainty of the method ( $1.08 \text{ nmol m}^{-2} \text{ s}^{-1}$  for  
186  $\text{H}_2$ ) and iii) the 95 % confidence interval (95% C.I.) of the HM model fit is less than 5 times the magnitude of  
187 the flux estimated using linear regression (removes poor-fitting outliers). In Figure 1 and Table 3, six examples  
188 are given in which three selections of linear regression fitting and three selections of the HMR model fitting  
189 are used to determine flux. For large uptake fluxes (Examples 4, 5 and 6) the HMR model provides a more  
190 suitable fit to the non-linearity in  $dC/dt$ , which linear regression does not accurately represent. Deposition  
191 velocity of  $\text{H}_2$  was calculated by dividing the calculated flux by the ambient concentration at the site (mean  
192 of  $t = 0$  measurements on day of measurement in  $\text{mol m}^{-3}$ ).

193



194

195 **Figure 1.** Examples of concentration data collected during  $\text{H}_2$  flux chamber sampling. Linear regression (grey)  
196 and HM model (brown) are used to determine  $dC/dt$  for each chamber measurement. Error bars represent  
197 the analytical uncertainty of  $\text{H}_2$  measurements by GC analysis (15 ppb in this study). Comparisons of flux data  
198 presented in Table 2.

199



200 **Table 2.** Further information on the example data provided in Figure 1. Six examples of chamber H<sub>2</sub> flux  
201 measurements are provided, from the Easter Bush (grassland) and Glencorse (woodland) field sites. The initial  
202 and final concentrations of H<sub>2</sub> within the chamber are provided, as well as the flux and 95% C.I. calculated  
203 using linear and HM model (Equation 2) fitting methods (NA when *k* is too large). The method selected to  
204 represent the flux in this study based on the described protocols is included.

Example	Date	Location	Initial (ppb)	Final (ppb)	Flux Linear fit (nmol m <sup>-2</sup> s <sup>-1</sup> )	Flux HM fit (nmol m <sup>-2</sup> s <sup>-1</sup> )	Selected Method
1	10/04/2024	Grassland	515	522	0.01 (-0.59 – 0.63)	2.839 (NA)	Linear
2	16/11/2023	Grassland	455	451	0.003 (-0.56 – 0.60)	0.239 (-6.47 – 6.99)	Linear
3	13/02/2024	Grassland	509	480	-0.319 (-0.58 – -0.06)	-0.889 (-2.60 – 0.21)	Linear
4	31/07/2024	Grassland	471	300	-3.078 (-4.54 – -3.35)	-6.6 (-9.44 – -3.80)	HM
5	31/07/2024	Grassland	483	229	-3.152 (-4.54 – -3.35)	-10.89 (-15.54 – -6.232)	HM
6	04/04/2024	Woodland	527	109	-5.278 (-7.05 – -1.07)	-14.35 (-15.88 – -12.82)	HM

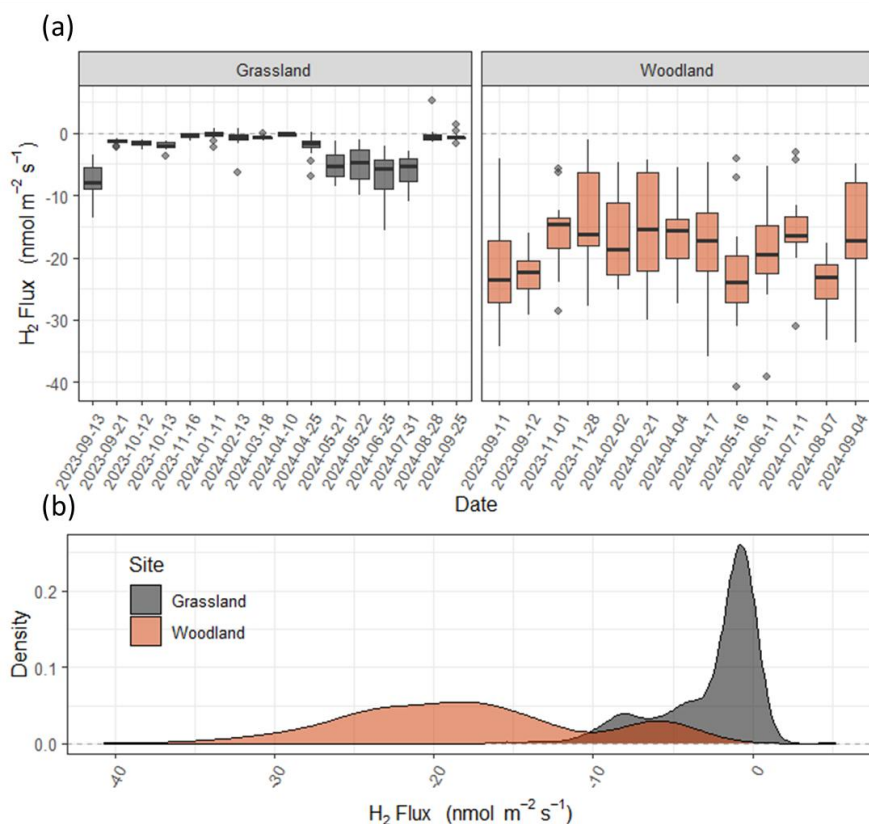
205

### 206 3. Results

#### 207 3.1. Hydrogen Flux measurements

208 Fluxes of H<sub>2</sub> measured from the grassland site ranged from -15.5 to +5.3 nmol m<sup>-2</sup> s<sup>-1</sup> (deposition velocity (V<sub>d</sub>)  
209 ranged from 0.070 to -0.026 cm s<sup>-1</sup>) (Figures 2 and S1) over the period of September 2023 to September 2024.  
210 More than 90% of the H<sub>2</sub> fluxes measured at the grassland site were negative (soil uptake) and only 2 of 251  
211 chamber measurements showed emissions from the soil which exceed the analytical uncertainty of the  
212 method. Fluxes of H<sub>2</sub> at the grassland site changed seasonally, with greater uptake in the spring and summer  
213 compared with winter, where the flux was close to zero. Fluxes at the grassland site had a median of -1.2 nmol  
214 m<sup>-2</sup> s<sup>-1</sup> and 95% percentiles of -9.9 to 0.2 nmol m<sup>-2</sup> s<sup>-1</sup>. Fluxes measured from the woodland site ranged from  
215 -40.7 to -1.1 nmol m<sup>-2</sup> s<sup>-1</sup> (V<sub>d</sub> ranged from 0.191 to 0.005 cm s<sup>-1</sup>) (Figures 2 and S1). All fluxes measured at the  
216 woodland site showed H<sub>2</sub> uptake in the soil. Spatial variability of H<sub>2</sub> flux at the woodland site was an order of  
217 magnitude larger than those observed at the grassland site. Fluxes at the woodland site had a median of -  
218 18.7 nmol m<sup>-2</sup> s<sup>-1</sup> and 95% percentiles of -32.4 to -4.3 nmol m<sup>-2</sup> s<sup>-1</sup>. Ambient concentrations of H<sub>2</sub> at the sites  
219 ranged from 424.8 to 566.5 ppb. Mean ambient concentrations at the woodland site (484.4 ppb) were on  
220 average 21.7 ppb (4.3 %) lower than the grassland site (506.5 ppb) which could be considered statistically  
221 insignificant (t-test, *p* > 0.1), but differences were fairly consistent throughout the year (summary statistics  
222 presented in Table S2).





223

224 **Figure 2.** Fluxes of H<sub>2</sub> measured using the flux chamber method at grassland (Easter Bush, grassland; grey)  
225 and forest (Glencorse Forest, woodland; red) sites in Midlothian, Scotland. Boxplots (a) represent the median,  
226 and 25<sup>th</sup> and 75<sup>th</sup> percentiles of flux data of 20 chambers, respectively (whiskers represent the 95<sup>th</sup>  
227 percentiles). (b) Frequency distributions of the flux data for both sites (Figure replicated for Vd in Figure S1).

### 228 **3.2. Greenhouse gas fluxes**

229 Fluxes of CH<sub>4</sub> at both sites were close to zero, with mostly small negative fluxes observed at both sites (Figure  
230 S3). Soil uptake of CH<sub>4</sub> was observed during the summer months at both sites but during colder months, only  
231 the woodland site continued to observe consistent negative CH<sub>4</sub> fluxes. Fluxes of CH<sub>4</sub> measured from the  
232 grassland site ranged from -1.2 to 1.0 nmol m<sup>-2</sup> s<sup>-1</sup> with a median of -0.14 nmol m<sup>-2</sup> s<sup>-1</sup>. Fluxes of CH<sub>4</sub> measured  
233 from the woodland site ranged from -1.3 to 2.3 nmol m<sup>-2</sup> s<sup>-1</sup> with a median of -0.32 nmol m<sup>-2</sup> s<sup>-1</sup>. Only 40% of  
234 all CH<sub>4</sub> flux measurements exceeded the analytical uncertainty of the chamber method deployed, highlighting  
235 the magnitude of observed fluxes were near the limit of detection of the methodology. Fluxes of N<sub>2</sub>O  
236 measured at both sites were relatively low for all measurement dates (58% of all data below the analytical



237 uncertainty) with the exception of measurements made in April at the grassland site. Nitrogen fertiliser was  
238 applied to the field on the 28<sup>th</sup> of March, resulting in increased N<sub>2</sub>O emissions for several weeks (Figure S3).

239

### 240 **3.3. Drivers of H<sub>2</sub> flux**

241 Correlations of H<sub>2</sub> flux with soil moisture and soil temperature can be observed at both sites (Figures 4a &  
242 4b); however, each site responds differently. Fluxes of H<sub>2</sub> at the grassland site were close to zero when water  
243 filled pore space (WFPS) was high (>45%), then tended towards uptake as WFPS decreased. The correlation  
244 between H<sub>2</sub> flux and WFPS is weaker at the woodland site and flux data are widely scattered. Fluxes of H<sub>2</sub> at  
245 both the grassland and woodland site tended towards higher uptake as temperature increased, though  
246 scatter increased toward higher uptake at both sites (>12 °C). A simplistic multiple regression fit between H<sub>2</sub>  
247 flux (y) with soil moisture (x) and soil temperature (z) ( $y = a_1x^2 + a_2x + b_1z^2 + b_2z + c$ ) accounts for more than  
248 half of the variance in the observed fluxes at the grassland site ( $R^2 = 0.60$ ) with a significant contribution from  
249 soil moisture, but the same approach does not adequately represent the large flux variability at the woodland  
250 site ( $R^2 = 0.14$ ) for which neither soil moisture or soil temperature was found to correlate significantly (Table  
251 S3). Fluxes of CH<sub>4</sub> at the sites followed the same trends as H<sub>2</sub> flux in terms of emission/uptake and follow  
252 similar correlations with soil moisture and soil temperature as H<sub>2</sub> flux (Figures 4c & 4d). Fluxes of CH<sub>4</sub> at both  
253 sites were close to zero (or emission) when soils were wet (>45 % WFPS) and cold (<6 °C). Uptake of CH<sub>4</sub> was  
254 greatest when soils were drier and warm.

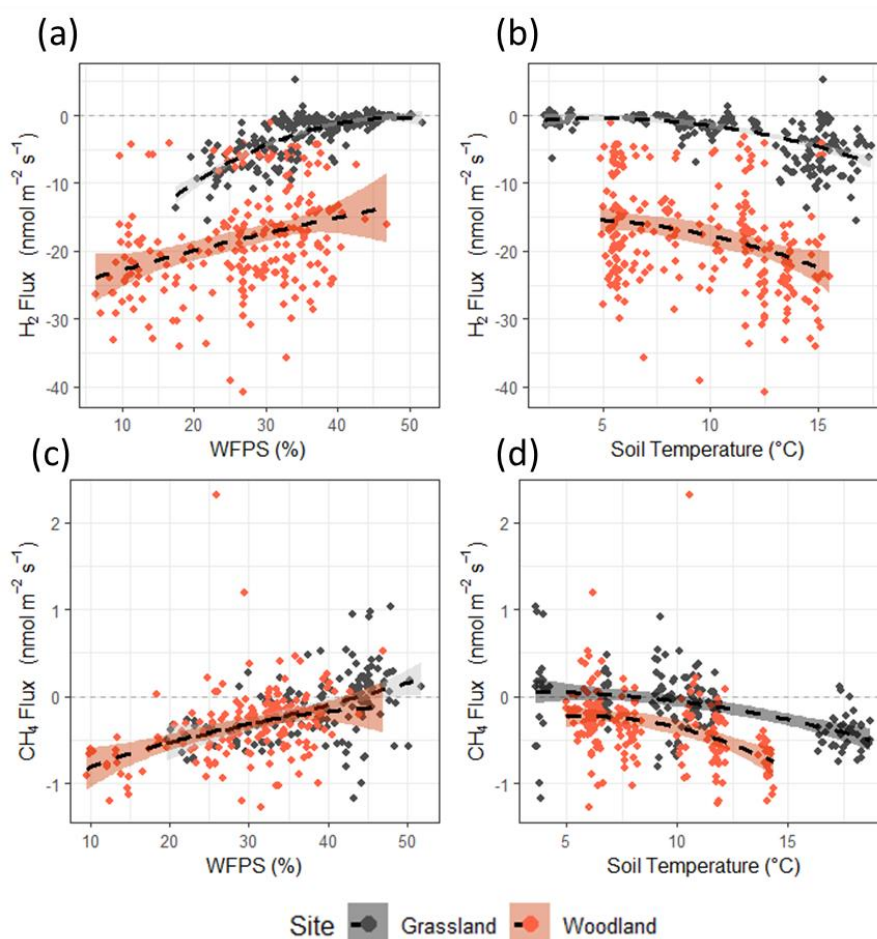
255 Total carbon (C) and total nitrogen (N) from the woodland site provided comparisons of H<sub>2</sub> flux with soil C and  
256 N at the chamber level (Figure S4). Variability in C and N in the replicated cores per chamber was similar to  
257 the magnitude of spatial variability at the plot scale, suggesting that localised soil samples were not  
258 adequately representative of the soil within a chamber (high spatial variability of C and N in the soil at the  
259 <1 m<sup>2</sup> scale). No correlation between H<sub>2</sub> flux with measured total soil C or N in the top 10 cm was found at  
260 the woodland site ( $R^2 < 0.01$  for each).

261 By combining continuous soil measurement data collected at each site (soil moisture and temperature at 10  
262 cm depth), with the multiple regression model with soil moisture and soil temperature (Figures 4b & 4c) as  
263 described in Table S1, continuous H<sub>2</sub> flux predictions were made for a full year (Figure 4a). This model predicts  
264 that H<sub>2</sub> flux at the grassland site remains close to zero for most of the time, except when soil moisture drops  
265 (e.g. warm months in spring and summer). The model predicts that H<sub>2</sub> flux at the grassland site is strongly  
266 dependent on the soil moisture content, with relatively strong periods of H<sub>2</sub> uptake during drier periods  
267 (warm periods between rainfall events). H<sub>2</sub> flux estimates at the woodland site are more variable, and less  
268 susceptible to changes in meteorology or soil conditions. The model predicts a slowdown in H<sub>2</sub> uptake in the



269 forest soils during the colder months in winter but is not significantly impacted by changing soil moisture.  
270 Total annual estimates of  $H_2$  flux predicted by the model are  $-3.1 \pm 0.1$  and  $-12.0 \pm 0.4$   $kg H_2 ha^{-1} yr^{-1}$  for the  
271 grassland and woodland sites, respectively. By comparison, a straight average of the measurements, without  
272 using models to gap-fill the data, suggests mean fluxes (with 95% C.I.s) of  $-2.6 \pm 0.4$  and  $-18.7 \pm 1.0$   $nmol m^{-2}$   
273  $s^{-1}$  which would translate to annual cumulative fluxes of approximately  $-1.6 \pm 0.2$  and  $-11.7 \pm 0.6$   $kg H_2 ha^{-1} yr^{-1}$   
274  $^1$  for the grassland and GC sites, respectively. The two estimates agree well at the woodland site, but the gap  
275 filling increases the estimated annual  $H_2$  uptake at the grassland site by 56%.

276



277

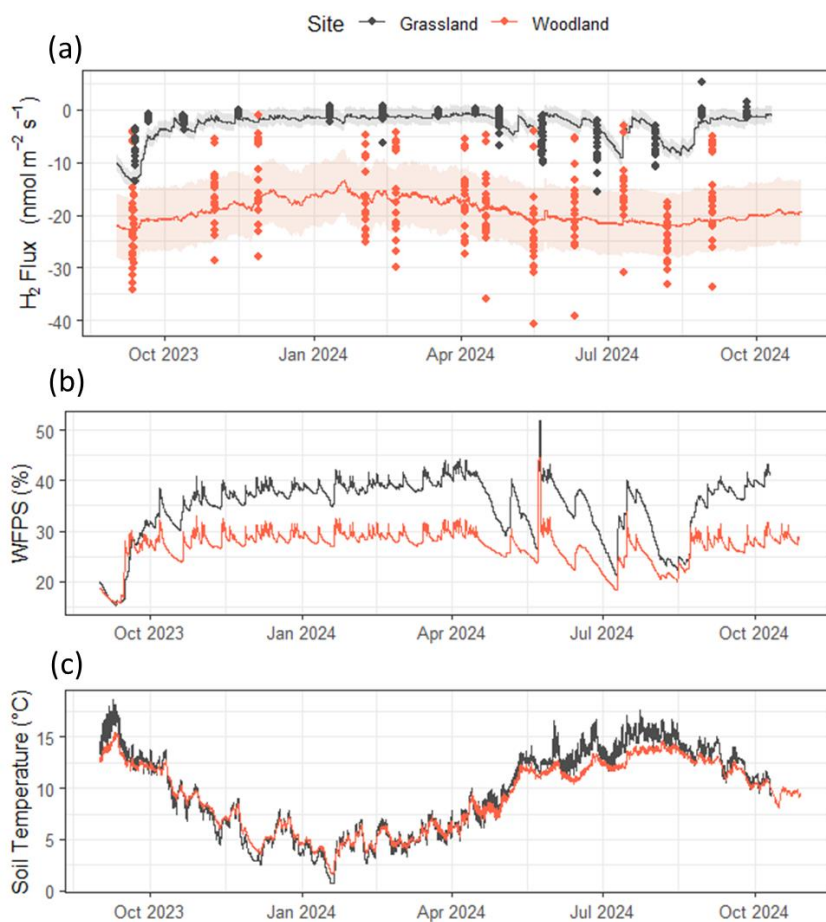
278

279 **Figure 3.** Correlations between  $H_2$  flux and (a) water filled pore space (WFPS) and (b) Soil Temperature.  
280 Correlations between  $CH_4$  flux and (c) water filled pore space (WFPS) and (d) Soil Temperature. WFPS and soil



281 temperature measured at 10 cm depth via sampling probe. A 2nd order polynomial fit (black dashed line) is  
282 included as a visual aid ( $y = a_1x^2 + a_2x + c$ ) (Figure replicated for Vd in Figure S2).

283



284

285 **Figure 4.** (a) H<sub>2</sub> flux measurements and model predictions for both field sites using a multiple regression fit  
286 with soil moisture ( $x$ ) and soil temperature ( $z$ ) ( $y = a_1x^2 + a_2x + b_1z^2 + b_2z + c$ ). (b) Continuous water filled pore  
287 space (WFPS) at measurements made at 10 cm depth (average of 60 mins). (c) Continuous soil temperature  
288 at measurements made at 10 cm depth (average of 60 mins).

289



## 290 4. Discussion

### 291 4.1. Quantification of H<sub>2</sub> flux

292 Fluxes of H<sub>2</sub> measured in this study range from -40.7 to 5.3 nmol m<sup>-2</sup> s<sup>-1</sup> with mean fluxes of -2.6 ± 0.4 and -  
293 18.7 ± 1.0 nmol m<sup>-2</sup> s<sup>-1</sup> for the grassland and woodland sites, respectively. Using regression to model (gap-fill)  
294 flux data, we estimate annual H<sub>2</sub> uptake of 3.1 ± 0.1 and 12.0 ± 0.4 kg H<sub>2</sub> ha<sup>-1</sup> yr<sup>-1</sup> for the grassland and  
295 woodland sites, respectively, which increases the expected mean uptake at the grassland site to 4.3 ± 0.2  
296 nmol m<sup>-2</sup> s<sup>-1</sup> while the expected mean uptake at the woodland site remains near 18 nmol m<sup>-2</sup> s<sup>-1</sup>. Predicted  
297 uptake is higher at the grassland site due to the expectation in the model that uptake will increase during  
298 periods of drier soils that were not measured directly. Predicted uptake estimated by the model and the  
299 extrapolation of the mean flux are not significantly different at the woodland site due to the lack of correlation  
300 with soil drivers in the model. However, the model does predict that uptake will slow down during the coldest  
301 months when fewer measurements were made at the site.

302 Mean measured uptake of H<sub>2</sub> at the grassland site is at the lower end of uptake reported in other studies that  
303 directly measured H<sub>2</sub> flux from soils, which range from -1.5 to >20 nmol m<sup>-2</sup> s<sup>-1</sup> (Table 3). The mean soil uptake  
304 of H<sub>2</sub> at the woodland site is at the higher end in terms of uptake magnitude, close in magnitude to high  
305 deposition velocities reported for peatlands in Simmonds et al., (2011). While uptake at this site seems high,  
306 we are confident that the flux measurements are accurate based on the consistency of flux observations and  
307 the quality controls put in place. Concentrations of H<sub>2</sub> in the chambers consistently fell exponentially, reaching  
308 near zero within 5 minutes (often within 3 mins) of enclosure. At the time of chamber closure (*t*<sub>0</sub>), a volume  
309 of 0.025 m<sup>3</sup> of ambient air at the woodland site contains approximately 400-500 nmol of H<sub>2</sub> gas. To reach zero  
310 within 5 mins would require fluxes approximately 10-12 nmol m<sup>-2</sup> s<sup>-1</sup> in magnitude. While dealing with the  
311 exponential non-linearity of the rate of change of the concentration (*dC/dt*) does introduce an element of  
312 uncertainty in the flux calculations, we are confident the method used in this study (HMR fitting) accurately  
313 captures the flux at *t*<sub>0</sub> and thus a realistic magnitude of soil H<sub>2</sub> uptake.

314 Only two of the measured H<sub>2</sub> fluxes were both positive and larger than the analytical noise of the  
315 measurement method. However, these measurements from separate chambers on separate dates (from the  
316 grassland site) both showed 7 consecutive concentration measurements, all clearly increasing with time,  
317 highlighting that it is possible for H<sub>2</sub> emissions to occur in soils, even where uptake is the predominant  
318 direction of flux. It has been observed that legumes produce H<sub>2</sub> during the nitrogen fixation process (e.g.  
319 Schubert and Evans 1976; Flynn et al., 2014); however, no legume plants were present in any of the chamber  
320 locations during the study. The source of these H<sub>2</sub> emissions remains unknown and at no point did either of  
321 the field sites become a source of H<sub>2</sub>, but our observations do highlight that there remain unknown microbial  
322 processes at the sub-field scale.



323 **Table 4.** A summary of H<sub>2</sub> fluxes and deposition velocity (Vd) measurements reported in literature, compared  
 324 with measured and modelled values in this study. Mean values and reported uncertainties. Where only flux  
 325 or Vd is reported, missing values are estimated using an ambient H<sub>2</sub> concentration of 500 ppb.

Study	Soil Type	Country	Mean H <sub>2</sub> Flux (nmol m <sup>-2</sup> s <sup>-1</sup> )	Mean Vd (cm s <sup>-1</sup> )
This study (measured)	Grass (Grazing)	UK (SCO)	-2.6 ± 0.4	0.012 ± 0.002
This study (gap-filled annual average)	Grass (Grazing)	UK (SCO)	-4.3 ± 0.2	
This study (measured)	Woodland	UK (SCO)	-18.2 ± 1.0	0.088 ± 0.005
This study (gap-filled annual average)	Woodland	UK (SCO)	-18.7 ± 0.6	
Smith-Downey et al. (2008)	Forest	USA (CA)	-7.9 ± 4.2	0.063 ± 0.029
	Desert	USA (CA)	-7.6 ± 5.3	0.051 ± 0.036
	Marsh	USA (CA)	-7.5 ± 3.4	0.035 ± 0.013
Lallo et al. (2009)	Urban park	FIN (Hesa)	-10.0 ± 2.5	0.020 ± 0.005
	Urban park	FIN (Hesa)	-19.0 ± 3.5	0.038 ± 0.007
Hammer and Levin (2009)	Urban/Agriculture	GER (BW)	-6.4 ± 1.6	0.03 ± 0.007
Simmonds et al. (2011)	Peatland	IRE (GAL)	26.5	0.053
			(9.0 – 64.5)	(0.018 – 0.129)
Meredith et al. (2017)	Woodland	USA (MA)	-3.2 ± 1.6	0.003 to 0.043
Baril et al. (2022)	Arable	CAN (QC)	-5.9 ± 4.3	0.012 ± 0.009
Buzzard et al. (2022)	Desert (Monsoon)	USA (AZ)	-1.5 to -3.5	0.03 to 0.007
Nagai et al. (2024)	Arable	JAP (JPO2)	-5 to -10	0.01 to 0.02

326

#### 327 **4.2. Drivers of H<sub>2</sub> flux**

328 This study provides evidence of large variability in H<sub>2</sub> flux behaviour across two different soil types and the  
 329 importance of environmental factors such as soil temperature and moisture content. At the grassland site,  
 330 soil moisture (WFPS) dominated the H<sub>2</sub> flux behaviour in the soils. The relationship between H<sub>2</sub> uptake and  
 331 soil moisture was statistically significant (p < 0.001) and explained 60% of the variance observed in the  
 332 grassland H<sub>2</sub> fluxes observed. While H<sub>2</sub> flux does appear to correlate with soil temperature at the grassland  
 333 site when compared directly, this is almost entirely due to the strong correlation between soil moisture and  
 334 soil temperature (R<sup>2</sup> = 0.68). Multiple regression finds soil temperature to be an insignificant variable once  
 335 the effect of soil moisture is accounted for at the grassland site. Spatial variability in H<sub>2</sub> fluxes at the woodland  
 336 site were an order of magnitude higher than those at the grassland site. This spatial variability could not be  
 337 explained by soil moisture, temperature or the total carbon content of the soil. While there do appear to be  
 338 weak relationships between the flux data and soil moisture and soil temperature, neither is found to be  
 339 statistically significant (maximum p-value of 0.15 for soil temperature).

340 Meteorological conditions were almost identical at the local scale (sites are less than 3 km apart) and soil at  
 341 both sites was of a similar pH and had similar total carbon and nitrogen contents. A small difference in



342 ambient H<sub>2</sub> concentrations was observed between the sites which may be caused by the large soil uptake and  
343 poorer circulation of air at the woodland site, resulting in lower near surface H<sub>2</sub> concentrations. The reason  
344 for the large difference in flux of H<sub>2</sub> measured between the two sites is not entirely clear from the measured  
345 data, but it is likely that the physical properties of the soils played a role. While rooting systems and carbon  
346 structure within the surface layers of the soils will be different at the sites, one large and obvious disparity is  
347 the clay content of the soils which is approximately 55% and 25% at the grassland and woodland sites,  
348 respectively. The higher density clay soil of the grassland site results in the soil becoming highly anaerobic  
349 when moisture levels increase, as can be seen in the switching from CH<sub>4</sub> uptake to CH<sub>4</sub> emission when WFPS  
350 exceeded 40%. At the woodland site, a thin layer of organic materials (forest litter) lies on top of a sandy, well-  
351 drained soil, which may provide ideal conditions for H<sub>2</sub> uptake. Uptake of CH<sub>4</sub> is generally greater than at the  
352 grassland site, and WFPS remains lower throughout the year, showing that drainage is significantly faster at  
353 the site and suggests that the soils are more aerobic than at the grassland site (e.g. better penetration of H<sub>2</sub>  
354 to active regions within the soil). While the differences in soil texture may partly explain the large magnitude  
355 of difference in H<sub>2</sub> uptake between the sites, it does not account for the large spatial variability of H<sub>2</sub> flux at  
356 the woodland site. While the flux at the grassland site is largely dependent on physical factors at the field  
357 scale such as the moisture content (aeration) of the soil, the woodland site showed large variations between  
358 plots. This variation may be due to microbial factors that are highly spatial in a forest floor, such as available  
359 nutrients (labile carbon from rotting plant litter), canopy shading and varying microbial densities.

360

#### 361 **4.3. Considerations for future research**

362 Chamber flux methods are commonplace in the field of GHG flux measurements, but there are several  
363 important factors that need to be considered when carrying out H<sub>2</sub> flux measurements in the field. One of  
364 the most important - when using gas chromatography analysis - is the lifetime of samples stored in vials.  
365 While it is possible to keep GHG samples in these vials for weeks or even months without significant storage  
366 loss, H<sub>2</sub> concentrations were found to change relatively quickly, and should be analysed as soon as is possible  
367 (within 24 h of measurement). This severely limits the reach of a particular field experiment to within travel  
368 distances of a working H<sub>2</sub> gas chromatography instrument (e.g. not suitable for international shipment of  
369 samples). Almost all published H<sub>2</sub> flux measurements to date are within the temperate region of the northern  
370 hemisphere (USA and Europe), which limits the available data for models to predict soil/atmosphere  
371 interactions at the global scale. Building H<sub>2</sub> flux datasets at a global level would require either investment in  
372 localised infrastructure that allows for samples to be analysed in-country, or for the deployment of temporary  
373 roving measurement methodology which travels between sites. We emphasise that unless particular care and



374 attention is applied to the transportation of gas samples (e.g. tests and quality control checks), the H<sub>2</sub> flux  
375 cannot be analysed over a large distance due to leakage of samples.

376 Field measurements of H<sub>2</sub> are beneficial due to realistic environmental conditions. However, the manual  
377 aspects of chamber sampling create logistical issues (extensive fieldwork) and the overlap of many  
378 environmental and soil variables can make it difficult to identify the driving forces behind H<sub>2</sub> flux (e.g. the soil  
379 moisture/temperature comparison). With this setup, the GC-PDHID is limited to one gas sample every 4  
380 minutes, thus auto-chambers (chambers that open/close and measure gas samples automatically) are limited  
381 in capability. New faster instruments able to measure H<sub>2</sub> gas via infra-red spectroscopy (by converting H<sub>2</sub> to  
382 H<sub>2</sub>O) are becoming more commercially available (see aerodyne.com/laser-analyzers), but there are no studies  
383 using these analysers to date. Previously gas chromatography instrumentation has been used to measure H<sub>2</sub>  
384 flux via the aerodynamic gradient method (Meredith et al., 2017), which allows half hourly fluxes to be  
385 measured at the field scale. While micrometeorological methods such as the aerodynamic gradient method  
386 allow for a greater temporal and spatial coverage of soil fluxes, they also require certain field conditions, such  
387 as flat open terrain and large (mains) power supply. In the case of the woodland site in this study,  
388 micrometeorological methods are not feasible. With current available H<sub>2</sub> measurement methods, care must  
389 be given when planning measurement activities to ensure efficiency in data collection.

390 Lab-based incubation studies of H<sub>2</sub> flux in literature are similar in number to those measured in the field.  
391 Incubation studies allow for better control of soil conditions such as moisture, temperature and nutrient  
392 content, environmental conditions (air temperature) and also for consistency in microbial populations (via  
393 replicates of well mixed/homogenised soils). For example, in this study, it was difficult to determine the  
394 impact of soil temperature due to the correlation with soil moisture. Due to the climate in the region, there  
395 were no periods when the soils were cold and also dry, preventing observations of different extremes of the  
396 driving forces behind H<sub>2</sub> flux. Incubation studies would be able to provide more information on these drivers  
397 which may help modelling efforts; however, field measurements are still required to validate flux models as  
398 incubation studies inevitably come with the caveat that flux measurements are not representative of true soil  
399 conditions due to soil cores being repacked and creating therefore artificial conditions.

## 400 **5. Conclusions**

401 This study reports that the soil sink (uptake) of H<sub>2</sub> for a grassland and a forest site in close proximity is  $-3.1 \pm$   
402  $0.1$  and  $-12.0 \pm 0.4$  kg H<sub>2</sub> ha<sup>-1</sup> yr<sup>-1</sup>, respectively (with mean V<sub>d</sub>s of  $0.012 \pm 0.002$  and  $0.088 \pm 0.005$  cm s<sup>-1</sup> for  
403 grassland and forest soils, respectively). Soil moisture was found to be the primary driver of H<sub>2</sub> uptake at the  
404 grassland site, where the high clay content of the soil resulted in anaerobic conditions (near zero H<sub>2</sub> flux)  
405 during wet periods of the year. Uptake of H<sub>2</sub> at the forest site was highly variable and did not correlate well





406 with any localised soil properties. Both sites were exposed to similar meteorological conditions (3 km apart)  
407 and had similar basic soil properties (such as pH and carbon content), thus we conclude that the large  
408 difference in uptake between the soils was dependent on soil aeration. It is likely that the high clay content  
409 of the grassland site (55%) resulted in a lack of aeration when soils were wet, while the well-drained forest  
410 site (25% clay) was not restricted by exchange of H<sub>2</sub> between the atmosphere and the soil, showing instead a  
411 large variability in H<sub>2</sub> flux that could be related to heterogeneous factors that control microbial activity (e.g.  
412 labile carbon and microbial densities). In order to account for the large magnitude of site-scale differences  
413 like those observed in this study, further field sites should be studied over a range of soil and land cover types  
414 and management activities to improve global models of the soil H<sub>2</sub> sink. In addition, laboratory incubations  
415 are needed to measure H<sub>2</sub> fluxes under controlled environmental conditions to refine the main driving  
416 parameters of H<sub>2</sub> fluxes further.

417

## 418 **6. Acknowledgements**

419 Funding for this study has been provided by the UKRI Natural Environment Research Council (NERC) under  
420 Grant Ref: NE/X013456/1 (Topic B: The Enigma of the Soil Hydrogen Sink Variability [ELGAR]). The work has  
421 also been supported by the UK Research and Innovation (UKRI) Global Challenges Research Fund (GCRF) as  
422 part of the South Asia Nitrogen Hub SANH project (NE/S009019/1).

423

## 424 **7. Competing interests**

425 The authors declare that they have no conflict of interest.

426

## 427 **8. Data availability**

428 Data currently undergoing preparation for submission to the Environmental Information Data Centre (EIDC).

429 <https://eidc.ac.uk/>

430



431 **9. Author contributions**

432 N. Cowan was the primary author of the manuscript and carried out all data analysis presented. The field  
433 team that developed measurement methodology protocols, carried out measurements, maintained field  
434 instrumentation and performed lab analysis consisted of T. Roberts, M. Hanlon, A. Bezanger, G. Toteva, A.  
435 Tweedie, K. Yeung and A. Deshpande. The project management and significant contributors to the  
436 manuscript text consisted of P. Levy, U. Skiba, E. Nemitz and J. Drewer. All coauthors contributed to the  
437 writing of the manuscript before submission.

438

439 **10. References**

- 440 Baril, X., Durand, A.-A., Srei, N., Lamothe, S., Provost, C., Martineau, C., Dunfield, K., Constant, P., 2022. The  
441 biological sink of atmospheric H<sub>2</sub> is more sensitive to spatial variation of microbial diversity than N<sub>2</sub>O and  
442 CO<sub>2</sub> emissions in a winter cover crop field trial. *Science of The Total Environment*.  
443 <https://doi.org/10.1016/j.scitotenv.2022.153420>
- 444 Bertagni, M.B., Pacala, S.W., Paulot, F., Porporato, A., 2022. Risk of the hydrogen economy for atmospheric  
445 methane. *Nat Commun.* <https://doi.org/10.1038/s41467-022-35419-7>
- 446 Billington, H.L. and Pelham, J., 1991. Genetic Variation in the Date of Budburst in Scottish Birch Populations:  
447 Implications for Climate Change. *Functional Ecology*, 5(3), pp. 403–409. <https://doi.org/10.2307/2389812>.
- 448 Buzzard, V., Thorne, D., Gil-Loaiza, J., Cueva, A., Meredith, L.K., 2022. Sensitivity of soil hydrogen uptake to  
449 natural and managed moisture dynamics in a semiarid urban ecosystem. *PeerJ*.  
450 <https://doi.org/10.7717/peerj.12966>
- 451 Conrad, R., 1999. Contribution of hydrogen to methane production and control of hydrogen concentrations  
452 in methanogenic soils and sediments. *FEMS Microbiology Ecology*. <https://doi.org/10.1111/j.1574-6941.1999.tb00575.x>
- 454 Cooper, J., Dubey, L., Bakkaloglu, S., Hawkes, A., 2022. Hydrogen emissions from the hydrogen value chain-  
455 emissions profile and impact to global warming. *Science of The Total Environment*.  
456 <https://doi.org/10.1016/j.scitotenv.2022.154624>
- 457 Cowan, N., Levy, P., Maire, J., Coyle, M., Leeson, S.R., Famulari, D., Carozzi, M., Nemitz, E., Skiba, U., 2020. An  
458 evaluation of four years of nitrous oxide fluxes after application of ammonium nitrate and urea fertilisers  
459 measured using the eddy covariance method. *Agricultural and Forest Meteorology*.  
460 <https://doi.org/10.1016/j.agrformet.2019.107812>



- 461 Derwent, R.G., Stevenson, D.S., Utembe, S.R., Jenkin, M.E., Khan, A.H., Shallcross, D.E., 2020. Global modelling  
462 studies of hydrogen and its isotopomers using STOICHEM-CRI: Likely radiative forcing consequences of a  
463 future hydrogen economy. International Journal of Hydrogen Energy.  
464 <https://doi.org/10.1016/j.ijhydene.2020.01.125>
- 465 Deshpande, A.G., Jones, M.R., van Dijk, N., Mullinger, N.J., Harvey, D., Nicoll, R., Toteva, G., Weerakoon, G.,  
466 Nissanka, S., Weerakoon, B., Grenier, M., Iwanicka, A., Duarte, F., Stephens, A., Ellis, C.J., Vieno, M., Drewer,  
467 J., Wolseley, P.A., Nanayakkara, S., Prabhawara, T., Bealey, W.J., Nemitz, E., Sutton, M.A., 2024.  
468 Estimation of ammonia deposition to forest ecosystems in Scotland and Sri Lanka using wind-controlled  
469 NH<sub>3</sub> enhancement experiments. Atmospheric Environment.  
470 <https://doi.org/10.1016/j.atmosenv.2023.120325>
- 471 Drewer, J., Anderson, M., Levy, P.E., Scholtes, B., Helfter, C., Parker, J., Rees, R.M., Skiba, U.M., 2016. The  
472 impact of ploughing intensively managed temperate grasslands on N<sub>2</sub>O, CH<sub>4</sub> and CO<sub>2</sub> fluxes. Plant Soil.  
473 <https://doi.org/10.1007/s11104-016-3023-x>
- 474 Drewer, J., Anderson, M., Levy, P.E., Scholtes, B., Helfter, C., Parker, J., Rees, R.M., Skiba, U.M., 2016. The  
475 impact of ploughing intensively managed temperate grasslands on N<sub>2</sub>O, CH<sub>4</sub> and CO<sub>2</sub> fluxes. Plant Soil.  
476 <https://doi.org/10.1007/s11104-016-3023-x>
- 477 Ehhalt, D.H., Rohrer, F., 2009. The tropospheric cycle of H<sub>2</sub>: a critical review. Tellus B: Chemical and Physical  
478 Meteorology. <https://doi.org/10.1111/j.1600-0889.2009.00416.x>
- 479 Field, R.A., Derwent, R.G., 2021. Global warming consequences of replacing natural gas with hydrogen in the  
480 domestic energy sectors of future low-carbon economies in the United Kingdom and the United States of  
481 America. International Journal of Hydrogen Energy. <https://doi.org/10.1016/j.ijhydene.2021.06.120>
- 482 Flynn, B., Graham, A., Scott, N., Layzell, D.B., Dong, Z., 2014. Nitrogen fixation, hydrogen production and N<sub>2</sub>O  
483 emissions. Can. J. Plant Sci. <https://doi.org/10.4141/cjps2013-210>
- 484 Greening, C., Grinter, R., 2022. Microbial oxidation of atmospheric trace gases. Nat Rev Microbiol.  
485 <https://doi.org/10.1038/s41579-022-00724-x>
- 486 Hammer, S., Levin, I., 2009. Seasonal variation of the molecular hydrogen uptake by soils inferred from  
487 continuous atmospheric observations in Heidelberg, southwest Germany. Tellus B: Chemical and Physical  
488 Meteorology. <https://doi.org/10.1111/j.1600-0889.2009.00417.x>
- 489 Hitchcock, W. K., Beamish, B. B. and Cliff D., 2019. A Study of the Formation of Hydrogen Produced During the  
490 Oxidation of Bulk Coal Under Laboratory Conditions, in Naj Aziz and Bob Kininmonth (eds.), Proceedings  
491 of the 2008 Coal Operators' Conference, Mining Engineering, University of Wollongong



- 492 Hutchinson, G.L., Mosier, A.R., 1981. Improved Soil Cover Method for Field Measurement of Nitrous Oxide  
493 Fluxes. Soil Science Society of America Journal.  
494 <https://doi.org/10.2136/sssaj1981.03615995004500020017x>
- 495 Islam, Z.F., Welsh, C., Bayly, K., Grinter, R., Southam, G., Gagen, E.J., Greening, C., 2020. A widely distributed  
496 hydrogenase oxidises atmospheric H<sub>2</sub> during bacterial growth. The ISME Journal.  
497 <https://doi.org/10.1038/s41396-020-0713-4>
- 498 Khalil, M.A.K., Rasmussen, R.A., 1990. The global cycle of carbon monoxide: Trends and mass balance.  
499 Chemosphere. [https://doi.org/10.1016/0045-6535\(90\)90098-e](https://doi.org/10.1016/0045-6535(90)90098-e)
- 500 Field, R.A., Derwent, R.G., 2021. Global warming consequences of replacing natural gas with hydrogen in the  
501 domestic energy sectors of future low-carbon economies in the United Kingdom and the United States of  
502 America. International Journal of Hydrogen Energy. <https://doi.org/10.1016/j.ijhydene.2021.06.120>
- 503 Lallo, M., Aalto, T., Hatakka, J., Laurila, T., 2009. Hydrogen soil deposition at an urban site in Finland. Atmos.  
504 Chem. Phys. <https://doi.org/10.5194/acp-9-8559-2009>
- 505 Meredith, L.K., Commane, R., Keenan, T.F., Klosterman, S.T., Munger, J.W., Templer, P.H., Tang, J., Wofsy, S.C.,  
506 Prinn, R.G., 2016. Ecosystem fluxes of hydrogen in a mid-latitude forest driven by soil microorganisms and  
507 plants. Global Change Biology. <https://doi.org/10.1111/gcb.13463>
- 508 Nagai, M., Kakiuchi, H., Masuda, T., 2024. Measurements of hydrogen deposition velocities by farmland soil  
509 using D<sub>2</sub> gas. Radiation Protection Dosimetry. <https://doi.org/10.1093/rpd/ncae055>
- 510 Novelli, P.C., Lang, P.M., Masarie, K.A., Hurst, D.F., Myers, R., Elkins, J.W., 1999. Molecular hydrogen in the  
511 troposphere: Global distribution and budget. J. Geophys. Res. <https://doi.org/10.1029/1999jd900788>
- 512 Ocko, I.B., Hamburg, S.P., 2022. Climate consequences of hydrogen emissions. Atmos. Chem. Phys.  
513 <https://doi.org/10.5194/acp-22-9349-2022>
- 514 Paulot, F., Paynter, D., Naik, V., Malyshev, S., Menzel, R., Horowitz, L.W., 2021. Global modeling of hydrogen  
515 using GFDL-AM4.1: Sensitivity of soil removal and radiative forcing. International Journal of Hydrogen  
516 Energy. <https://doi.org/10.1016/j.ijhydene.2021.01.088>
- 517 Paulot, F., Pétron, G., Crotwell, A.M., Bertagni, M.B., 2024. Reanalysis of NOAA H<sub>2</sub> observations: implications  
518 for the H<sub>2</sub> budget. Atmos. Chem. Phys. <https://doi.org/10.5194/acp-24-4217-2024>
- 519 Patterson, J.D., Aydin, M., Crotwell, A.M., Pétron, G., Severinghaus, J.P., Krummel, P.B., Langenfelds, R.L.,  
520 Saltzman, E.S., 2021. H<sub>2</sub> in Antarctic firn air: Atmospheric reconstructions and implications for  
521 anthropogenic emissions. Proc. Natl. Acad. Sci. U.S.A. <https://doi.org/10.1073/pnas.2103335118>



- 522 Pedersen, A.R., Petersen, S.O., Schelde, K., 2010. A comprehensive approach to soil-atmosphere trace-gas  
523 flux estimation with static chambers. *European J Soil Science*. <https://doi.org/10.1111/j.1365->  
524 2389.2010.01291.x
- 525 Petron, G. B., Crotwell, A. M., Mund, J., Crotwell, M., Mefford, T., Thoning, K., Hall, B. D., Kitzis, D. R.,  
526 Madronich, M., Moglia, E., Neff, D., Wolter, S., Jordan, A., Krummel, P., Langenfelds, R., and Patterson, J.  
527 D.: Atmospheric H<sub>2</sub> observations from the NOAA Global Cooperative Air Sampling Network, *Atmos. Meas.*  
528 *Tech. Discuss.* [preprint], <https://doi.org/10.5194/amt-2024-4>, in review, 2024.
- 529 Piché-Choquette, S., Constant, P., 2019. Molecular Hydrogen, a Neglected Key Driver of Soil Biogeochemical  
530 Processes. *Appl Environ Microbiol*. <https://doi.org/10.1128/aem.02418-18>
- 531 Saavedra-Lavoie, J., de la Porte, A., Piché-Choquette, S., Guertin, C., Constant, P., 2020. Biological H<sub>2</sub> and CO  
532 oxidation activities are sensitive to compositional change of soil microbial communities. *Can. J. Microbiol.*  
533 <https://doi.org/10.1139/cjm-2019-0412>
- 534 Sand, M., Skeie, R.B., Sandstad, M., Krishnan, S., Myhre, G., Bryant, H., Derwent, R., Hauglustaine, D., Paulot,  
535 F., Prather, M., Stevenson, D., 2023. A multi-model assessment of the Global Warming Potential of  
536 hydrogen. *Commun Earth Environ*. <https://doi.org/10.1038/s43247-023-00857-8>
- 537 Schubert, K.R., Evans, H.J., 1976. Hydrogen evolution: A major factor affecting the efficiency of nitrogen  
538 fixation in nodulated symbionts. *Proc. Natl. Acad. Sci. U.S.A.* <https://doi.org/10.1073/pnas.73.4.1207>
- 539 Simmonds, P.G., Derwent, R.G., Manning, A.J., Grant, A., O'doherty, S., Spain, T.G., 2011. Estimation of  
540 hydrogen deposition velocities from 1995–2008 at Mace Head, Ireland using a simple box model and  
541 concurrent ozone depositions. *Tellus B: Chemical and Physical Meteorology*.  
542 <https://doi.org/10.1111/j.1600-0889.2010.00518.x>
- 543 Smith-Downey, N.V., Randerson, J.T., Eiler, J.M., 2008. Molecular hydrogen uptake by soils in forest, desert,  
544 and marsh ecosystems in California. *J. Geophys. Res.* <https://doi.org/10.1029/2008jg000701>
- 545 Warwick, N.J., Bekki, S., Nisbet, E.G., Pyle, J.A., 2004. Impact of a hydrogen economy on the stratosphere and  
546 troposphere studied in a 2-D model. *Geophysical Research Letters*. <https://doi.org/10.1029/2003gl019224>
- 547
- 548